
# Unveiling the building embodied carbon dynamics in Yangtze River Delta: Spatial and life cycle perspectives



Citation for the original published paper (version of record):
Liang, H., Zhang, B., Bian, X. et al (2025). Unveiling the building embodied carbon dynamics in Yangtze River Delta: Spatial and life cycle
perspectives. Journal of Urban Management, 14(1): 160-180.
http://dx.doi.org/10.1016/j.jum.2024.10.004

Journal of Urban Management 14 (2025) 160–180

HOSTED BY

Contents lists available at ScienceDirect

Journal of Urban Management

journal homepage: www.elsevier.com/locate/jum

Research Article

# Unveiling the building embodied carbon dynamics in Yangtze River Delta: Spatial and life cycle perspectives

Hanwei Liang [a], Baizhe Zhang [a], Xin Bian [a,b], Jieling Shen [a], Yuxuan Wang [a], Liang Dong [c,d,e,*]

[a] Collaborative Innovation Center on Forecast and Evaluation of Meteorological Disasters/Research Center of Urban Sustainable Development/School of Geographical Sciences, Nanjing University of Information Science & Technology (NUIST), Nanjing, 210044, China
[b] Department of Architecture and Civil Engineering, Chalmers University of Technology, SE-41296, Gothenburg, Sweden
[c] Department of Public and International Affairs (PIA), City University of Hong Kong, Hong Kong SAR, China
[d] School of Energy and Environment (SEE), City University of Hong Kong, Hong Kong SAR, China
[e] Centre for Public Affairs and Law, City University of Hong Kong, Hong Kong SAR, China

ARTICLE INFO

*Keywords:*
Building material stock
Embodied carbon emission
Nighttime lights
Life cycle assessment
Construction materials
Yangtze river Delta

ABSTRACT

Understanding and reducing the greenhouse gas emissions from building sector is significant to realize the net zero society. This research presents a bottom-up approach leveraging nighttime light (NTL) data to quantitatively assess and spatially represent urban building Material Stock (MS) and Embodied Carbon Emissions (ECE) throughout the "cradle-to-gate" lifecycle, at the micro-unit level, within the rapidly urbanizing Yangtze River Delta (YRD) region. Our primary focus is on investigating the dynamics and evaluating the impacts of building material stocks and the associated embodied carbon under urban expansion. Key findings include: (1) From 2000 to 2020, the YRD experienced a significant increase in building MS, with development expanding more rapidly along the southeast-northwest axis than the southwest-northeast axis. (2) Building ECE grew markedly in the YRD, especially in coastal areas, shifting from a concentrated single-center pattern to a multi-center one. The growth trends of building ECE among these cities varied widely, ranging from 0.64 to 85.71 Tg per year (Tg/a). (3) Construction materials such as sand, gravel, cement, and brick dominated the MS in both residential and non-residential buildings. Cement, steel, brick, and aluminum were the main contributors to building ECE. Notably, despite their lower volumes, copper and aluminum had substantial environmental impacts due to their high ECE contributions. (4) By categorizing cities into four types based on ECE per capita and growth trends, we identified varied urban development and environmental impacts across the YRD.

## Abbreviations

| | |
|---|---|
| MS | Material stock |
| ECE | Embodied carbon |
| YRD | Yangtze River Delta |
| NTL | Nighttime light |

(*continued on next page*)

* Corresponding author. Department of Public and International Affairs (PIA), City University of Hong Kong, Hong Kong, SAR, Hong Kong, China.
*E-mail addresses:* liang.hanwei@nuist.edu.cn (H. Liang), zhang.baizhe@nuist.edu.cn (B. Zhang), xinb@chalmers.se (X. Bian), shen.jieling@nuist.edu.cn (J. Shen), wang.yuxuan@nuist.edu.cn (Y. Wang), liadong@cityu.edu.hk (L. Dong).

https://doi.org/10.1016/j.jum.2024.10.004
Received 17 May 2024; Received in revised form 11 October 2024; Accepted 15 October 2024
Available online 30 October 2024

(*continued*)

| | |
|---|---|
| GIS | Geographic information systems |
| LCA | Lifecycle assessment |
| MI | Material intensity |
| BUA | Built-up area cells |
| EF | Carbon emission factors |
| OSM | OpenStreetMap |
| SDE | Standard Deviational Ellipse |
| DMSP/OLS | Defense Meteorological Satellite Program/Operational Line Scan |
| NGDC | National Geophysical Data Center |
| NOAA | National Oceanic and Atmospheric Administration |
| S-NPP VIIRS | Suomi National Polar-orbiting Partnership Visible Infrared Imaging Radiometer Suite |
| Tg | Teragrams |

## 1. Introduction

Addressing climate change and fostering urban sustainability have emerged as urgent global priorities, and urban built environment is a critical field. As cities expand and populations concentrate, there is a substantial increase in resource consumption and carbon emissions associate with the expansion of built environment. This trend is particularly pronounced in rapidly urbanizing nations such as China, where urban areas contributed over 70% of the country's carbon emissions in 2020, marking a substantial increase from 1980 levels (Wang et al., 2023; Zheng et al., 2024). The building sector, as a key component of urban built environment, and therefore as a major contributor to urban carbon emissions, underscores the critical need for focused research on its environmental impacts and mitigation strategies (Liu et al., 2023; Zhou et al., 2022). To effectively address these issues, a comprehensive framework for managing urban built environment and building sector is essential (Bai et al., 2018; Seto et al., 2017).

Urban metabolism provides such a framework by offering a comprehensive perspective to examine the flows of materials, energy, and waste within cities. This concept is crucial for understanding the complexities of urban sustainability and for developing effective climate change mitigation strategies. By analyzing these flows, urban metabolism helps identify key opportunities to minimize environmental impacts and enhance sustainability (Kennedy et al., 2007). In this context, focusing on urban building Material Stock (MS) and Embodied Carbon Emissions (ECE) becomes particularly important. These metrics not only represent the accumulation and lifecycle impacts of construction materials like concrete, steel, and timber, but also highlight their significant contributions to a city's carbon footprint, emphasizing the need for sustainable building practices (Tanikawa & Hashimoto, 2009; You et al., 2011).

The Yangtze River Delta (YRD) region, characterized by rapid urbanization, serves as a critical case study for examining the dynamics of urban material stock and carbon emissions. Situated at the mouth of the Yangtze River, the YRD is a major economic hub with unique river-sea transport capabilities, acting as a vital gateway for China's international trade and economic activities. This rapid development has led to extensive urban expansion, significantly increasing the consumption of building materials and the associated carbon emissions (Gu et al., 2011; Han et al., 2016; Zhong et al., 2024). Therefore, understanding the complex material flows and carbon dynamics within the YRD is essential for informing sustainable urban practices and climate change mitigation strategies at both national and global levels (Zhang, L. et al., 2022; Zheng et al., 2016). By delving into these aspects, our study highlights the YRD's pivotal role in advancing urban sustainability and addressing broader environmental challenges.

This study aims to explore the dynamics of both metallic and non-metallic construction materials in the YRD region by utilizing nighttime light (NTL) data to quantitatively analyze and spatially map MS and ECE at a micro-unit scale from 2000 to 2020. The specific objectives are: (1) to map the spatial and temporal variations in building MS and ECE, enhancing understanding of how urban material stock and carbon emissions evolve over time; (2) to conduct a detailed comparison of the impacts associated with different building materials, specifically contrasting metallic materials like steel, copper, and aluminum against non-metallic materials such as asphalt, brick, and cement; and (3) to generate targeted strategies that mitigate the environmental impacts of these materials in support of sustainable urban development. By employing a combination of geographic information systems (GIS) and lifecycle assessment (LCA) methodologies, this research provides a comprehensive bottom-up analysis from the “cradle to gate” stage, offering insights that could inform both local policy decisions and broader sustainable urban management practices, particularly in other rapidly urbanizing regions worldwide.

## 2. Literature review

### 2.1. Urban metabolism and material stock

Urban metabolism provides a foundational framework for understanding the complex system of flows and processes involved in the production, consumption, and disposal of resources within cities. It integrates both the physical and social dimensions of urban life, offering a comprehensive view of how cities operate as integrated systems (Gandy, 2004; Kennedy et al., 2007). By examining the flows of materials, energy, and waste, this concept highlights the sustainability challenges and resource management issues inherent in rapidly urbanizing areas (Bai, 2016; Kennedy et al., 2011).

Central to the concept of urban metabolism is MS, which embodies the accumulated resources and infrastructure within cities—such

as buildings, roads, and utilities—that significantly influence their environmental impact, resource efficiency, and long-term sustainability (Niza et al., 2009; Tanikawa & Hashimoto, 2009). As urban areas expand, the dynamics of MS become a key determinant of their resource demands and carbon emissions. Understanding and strategically managing this stock is crucial for enhancing urban sustainability, making it imperative to monitor and innovate ways to optimize resource use and minimize environmental footprints over time (Tanikawa et al., 2002).

Previous studies on urban MS have increasingly focused on the accumulation and distribution of resources and infrastructure within cities, revealing significant implications for environmental sustainability and urban development patterns (González & Navarro, 2006; Krausmann et al., 2009). These investigations highlight the direct link between the growth of MS and increased resource consumption and waste generation, underscoring the necessity for sustainable urban planning and optimized material use (Augiseau & Barles, 2017; Lehmann, 2011). As urban areas, particularly in rapidly developing regions, continue to expand, managing MS becomes crucial for balancing economic growth with environmental protection (Wiedenhofer et al., 2019).

In addressing these challenges, current MS accounting methods are generally divided into "top-down" and "bottom-up" approaches, each with distinct challenges and limitations (Müller, 2006). The top-down approach relies on macro-level socio-economic data to estimate MS by calculating the accumulated differences between inflows and outflows. Despite its utility for broad analyses, this method often faces limitations due to issues of data availability, scale, and timeliness, which hinder its effectiveness at urban and sub-urban scales where precise and current data are vital for accurate assessments (Schiller et al., 2017; Tanikawa et al., 2015). Conversely, the bottom-up approach leverages detailed product or infrastructure-level statistics, aggregating them upwards. This method has evolved to incorporate three-dimensional GIS data combined with material intensity (MI) metrics for conducting more granular, urban-scale analyses. However, the dependency on advanced GIS data—often costly and primarily available in developed regions—poses significant barriers to its widespread application, especially in less developed areas where such data may be scarce (Pauliuk et al., 2012).

Recently, NTL remote sensing technology has become a significant tool for monitoring urban resources and the environment, offering numerous advantages for studying urban metabolism. NTL provides spatially explicit data that can effectively map urban MS, monitor temporal changes, and cover extensive areas at relatively low cost, making it particularly useful in regions lacking traditional data sources (Elvidge et al., 2017; Zhang & Seto, 2011). The integration of NTL data with GIS allows for the detailed spatialization of MS data at finer grid scales, enhancing the analysis of urban material distribution and dynamics (Haberl et al., 2021; Peled & Fishman, 2021; Vilaysouk et al., 2021).

However, despite the advancements in remote sensing and GIS technologies, challenges remain in the longitudinal spatialization of MS at the urban micro-unit scale. Existing studies have begun to address these gaps by employing bottom-up MS accounting methods based on NTL, which have provided insightful analyses across various scales and periods (Hattori et al., 2014; Hsu et al., 2013; Liang et al., 2014, 2017). Yet, there is still a critical need for methods that can capture the detailed temporal and spatial heterogeneity of MS within cities to better understand and manage urban metabolism for sustainable development. Our team's recent work has proposed a novel approach that segments cities into built-up area cells (BUA), allowing for the estimation of building MS over extended periods at this granular scale, thereby providing a methodological foundation for in-depth urban micro-unit scale MS analysis (Liang et al., 2023c).

### *2.2. LCA and Embodied Carbon Emissions*

LCA is an advanced and well-recognized approach for evaluating the environmental impacts of products and services throughout their entire life cycle, defined as stages from raw material extraction to production, use, disposal and waste management (Cui et al., 2011; Pandit et al., 2017). This comprehensive approach has been instrumental in urban metabolism studies, providing a holistic view of the environmental burdens associated with urban systems and identifying strategies for reducing these impacts (Finnveden et al., 2009; ISO-Norm, 2006, p. 157). A crucial aspect of LCA in urban contexts is the analysis of ECE, which quantifies the total carbon emissions from construction materials across their life cycle stages: cradle (extraction), gate (production), site (transportation), endpoint (operation), grave (disposal), and cradle again (recycling) (Hammond & Jones, 2008). The cradle-to-gate stage is particularly significant as it encompasses emissions from material extraction up to the point they leave the production facility, representing a major portion of the lifecycle emissions and offering substantial opportunities for reducing the carbon footprint of urban development (Cabeza et al., 2014).

ECE analysis can be conducted at various scales, ranging from individual buildings or clusters to broader urban, regional, or national levels (Table 1). At larger scales, methodologies that combine LCA with MS data allow for the efficient aggregation of data, providing macro-level insights into ECE. However, these large-scale analyses often lack the granularity required for detailed regional studies, which is crucial for developing targeted sustainability strategies and understanding spatial and temporal dynamics of ECE (Acquaye et al., 2011; Kaoula and Bouchair, 2018, 2020; Suh et al., 2004). By integrating LCA with detailed MS data, the precision of ECE assessments is enhanced, especially at the urban scale, allowing for more accurate evaluations of cradle-to-gate emissions (Pauliuk et al., 2012).

Our study advances this approach by linking MS data with carbon emission factors (EF), providing a detailed analysis of the carbon impacts of specific construction materials over extended periods. By incorporating bottom-up and LCA methodologies, we bridges the gap between managing extensive datasets and the need for precise, actionable environmental impact information (Chen et al., 2017; Lavagna et al., 2018; Liang et al., 2023b; Zheng et al., 2023).

While recent studies on the cradle-to-gate emissions stage of MS and ECE at the micro-unit scale have provided valuable insights into the environmental impacts of urban systems, significant gaps remain. Most existing research has overlooked variations in building types within cities, often neglecting the estimation and longitudinal mapping of building-specific ECE at the micro-unit scale. This oversight limits our ability to develop targeted sustainability strategies that consider the unique material compositions and associated carbon

**Table 1**
Literature review of building ECE.

| Scale | Methodology | | Method | Data | LCA stage coverage | Reference |
|---|---|---|---|---|---|---|
| Single building | Bottom-up | ● | LCA method (three single-family buildings in Okanagan, British and Columbia, Canada in 2018) | Census data (energy consumption and construction materials of buildings) | Cradle to gate | Kamali et al. (2019) |
| | | ● | Inventory analysis of different construction materials (single building at Curtin University in Western Australia in 2013) | Inventory data (input and output data, including energy consumption and types, distance, amount of construction materials) | Cradle to site | Biswas (2014) |
| | | ● | Life-cycle inventory and impact assessment (single-storey retail building in Toronto, Canada in 2011) | Inventory data (types and quantities of building component) | Cradle to grave | Van Ooteghem and Xu (2012) |
| | | ● | BIM-LCA integrated method (one residential tower in Aalborg, Denmark in 2022) | Inventory data (floor area, building shape and energy consumption of buildings) | Cradle to grave | Felicioni et al. (2023) |
| | | ● | LCA method (three types of hotel buildings in Algeria and France) | Inventory data (energy consumption of buildings) | | Kaoula and Bouchair (2018) |
| | | ● | LCA method and sensitivity analysis (five ecological houses) | Inventory data (geometry, climate zones, envelopes and energy consumption of buildings) | | Kaoula and Bouchair (2020) |
| Building cluster | Bottom-up | ● | Descriptive statistics analysis, correlation analysis and goodness-of-fit test (43 buildings in Korea in 2014) | Inventory data (gross floor area types, building structure types of buildings and types and embodied carbon of building materials) | Cradle to site | Kang et al. (2015) |
| | | ● | Inventory analysis and statistical analysis (403 residential buildings in China in 2020) | Inventory data (number of floors, height, gross floor area of buildings, types, weight, intensity transport distance and emission factors of building materials) | Cradle to site | Zhang et al. (2023) |
| | | ● | WLCE calculation method and correlation analysis (145 residential buildings in Cornwall, UK in 2020) | Survey data (age, construction type, yearly energy consumption and carbon intensity of buildings, types, quantities, transport distances and emission factors of building materials) | Cradle to grave | Zheng et al. (2023) |
| Urban | Bottom-up | ● | Spatial and socioeconomic analysis (urban buildings in Beijing, China in 2018, including public, residential, commercial and educational buildings) | Spatial data (GIS data and spatial distribution data) and statistical data (physical size of construction sector, material intensity, embodied GHG emission factor of construction materials) | Cradle to gate | Mao et al. (2020) |
| | Top-down | ● | Spatial disparity analysis and decoupling analysis (buildings in Shanghai, China from 2000 to 2016, including residential and non-residential buildings) | Inventory data (types, mass, material intensity and unit embodied GHG emissions of construction materials, building area, building types) | Cradle to gate | Huang et al. (2019) |
| | | ● | Statistical analysis (district buildings in Guangzhou, China in 2020, including high-rise office, hotel and residential buildings) | Inventory data (types, consumption, average transportation distance and carbon emission factor of construction materials) | Cradle to grave | Pan et al. (2023) |
| Regional | Bottom-up | ● | BSM and BEM (urban residential buildings in New York state, USA in 2021) | Spatial data (GIS data, tax parcel, building footprints and LiDAR point clouds) and inventory data (construction year, construction materials and carbon emission coefficient) | Cradle to gate | Heisel et al. (2022) |
| | Top-down | ● | BIM (urban buildings in Greater Bay Area, China in 2018, including residential and non-residential buildings) | Inventory data (types, mass, average distance and unit carbon emission of construction materials) | Cradle to site | Peng et al. (2021) |
| | | ● | LCA method and statistical analysis (residential buildings of the EU in 2010, including 24 types of statistically-based residential buildings) | Statistical data (magnitude of the building stock, the periods of construction, the physical characteristics, and the energy consumption) | Cradle to grave | Lavagna et al. (2018) |
| National | Top-down | ● | Carbon forecast equation and linear optimization modeling (residential buildings in Nepal in 2021) | Census data (counts of materials utilized in each household with detailed breakdown of building components used by the foundation, wall, floor, and roof and carbon emission coefficient) | Cradle to gate | Paneru et al. (2024) |
| | | ● | Statistical analysis (buildings in China in 2021, including residential, industrial and public buildings) | Statistical data (floor areas of buildings, material intensity, embodied energy coefficient and types of construction materials) | Cradle to site | Chen et al. (2022) |
| | Bottom-up | ● | A four-step bottom-up modeling approach (residential building stock in USA in 2018) | Spatial data (GIS) and statistical data (building types, foundation types, number of stories, wall structure types, wall materials, roofing materials, window types/numbers, floor areas, number of bedrooms and building height) | Cradle to grave | Hu (2023) |

emissions of different building types, which are crucial for enhancing urban sustainability (Giesekam et al., 2014; Moncaster & Symons, 2013).

Furthermore, detailed analyses comparing the ECE of metallic versus non-metallic materials are scarce. Comprehensive studies that cover the entire lifecycle of these materials within buildings—and their contributions to the overall urban carbon footprint—are also lacking. Such research is vital to fully understand the environmental impacts of different material types and to inform the development of sustainable construction practices (Cabeza et al., 2014; Häfliger et al., 2017). Additionally, there is a need for more integrated studies that combine MS and ECE data to analyze urban development patterns and propose sustainable policies. Integrating these aspects is crucial for developing a holistic approach to urban sustainability, as it allows for a better understanding of how material use and carbon emissions are interconnected and can be managed to promote sustainable urban growth (Huang et al., 2019; Müller et al., 2013; Zhang, N. et al., 2022).

### 2.3. Relevant research on YRD

YRD in eastern China is a region of great significance due to its large population and rapid economic growth. As one of China's major economic hubs, it experiences intense urbanization and industrial activity, leading to significant environmental challenges (An et al., 2021; Qiao & Huang, 2022; Zhao et al., 2016). Cities like Shanghai, Nanjing, and Hangzhou are part of this region, making it an ideal case study for exploring the complex interactions between urban expansion, resource consumption, and environmental sustainability. Researchers have extensively explored the YRD's urbanization processes, examining their impacts on resource consumption and environmental indicators such as $PM_{2.5}$ and $CO_2$ emissions, employing various methodologies including spatial autoregressive models and environmental Kuznets curve theory to assess the effects of land, population, and economic urbanization dynamics across the region (Cheng et al., 2020; Zhao et al., 2016; Zhong et al., 2024; Zhou et al., 2019).

Despite these efforts, there has been insufficient focus on the dynamics of building stock and its cradle-to-gate emissions stage within the YRD. Understanding these factors is crucial for comprehending the full environmental impact of urban infrastructure (Chen et al., 2023; Han et al., 2016). The cradle-to-gate stage involves the extraction, production, and transportation of construction materials, which

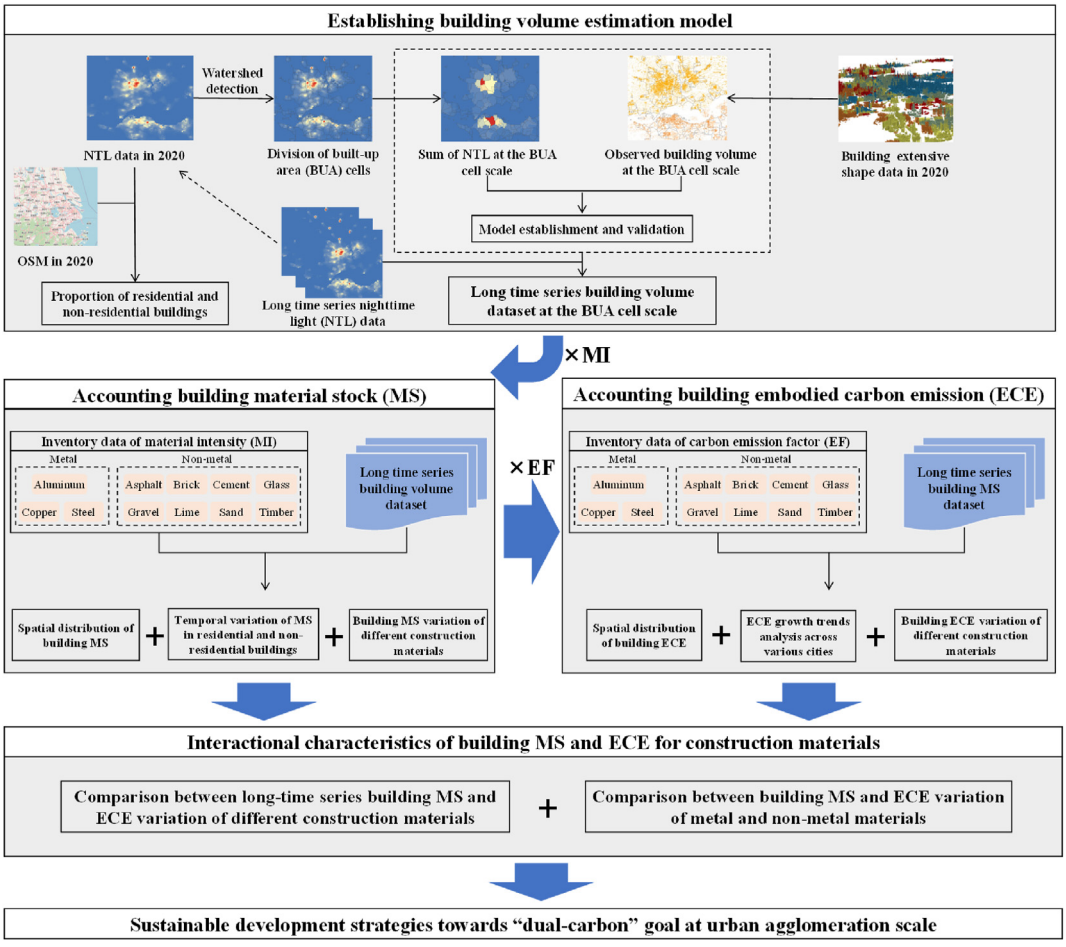


**Fig. 1.** Framework of calculation procedure.

significantly contribute to the carbon footprint of urban development. While current research emphasizes the need for sustainable urban planning and construction practices, it often overlooks these critical emission stages, leaving a gap in our comprehensive understanding of environmental impacts (Gu et al., 2011).

Moreover, detailed analyses of the long-term temporal dynamics and spatial variations of MS and ECE in the YRD are scarce. The region's uneven growth poses unique challenges for accurately mapping material stock and carbon emissions across different urban settings over time (Zhou et al., 2019). Our study aims to address these gaps by focusing on a detailed examination of building stock and its associated cradle-to-gate emissions, taking into account the diverse nature of urban development across the YRD. By building on previous research, including the work of Bai and Qu (2021) and (Liang et al., 2023b), our study integrates LCA and MS data to uncover micro-scale ECE dynamics that are often overlooked in broader studies. This approach enhances the accuracy of ECE assessments and provides essential data for developing targeted sustainability strategies in the YRD, a region marked by rapid urbanization and significant material turnover. Through this comprehensive analysis, our research contributes to the development of targeted policies that support sustainable, low-carbon urban development, thereby aiding broader regional and global efforts to mitigate climate change.

## 3. Methodology

The methodology employed in this study is structured around three main procedures, with the entire calculation framework depicted in Fig. 1. The spatial boundary of this research is defined as the Yangtze River Delta (YRD) urban agglomeration, as shown in Fig. 2. Initially, we utilized NTL data and GIS data in 2020 to develop a model for estimating building volume. This model was then applied to assess the building volume within the built-up areas of YRD over a twenty-year period, from 2000 to 2020. Following the establishment of this model, we proceeded to calculate the building MS in the YRD for the same period, employing the material intensity (MI) values of various construction materials. Finally, by incorporating carbon emission factors (EF), we leveraged the building MS data to estimate the building ECE for the "cradle to gate" stage in the YRD from 2000 to 2020, achieving a comprehensive spatialization of building MS and ECE over this extended timeframe.

### 3.1. Establishment of building volume estimation model

Our methodology for establishing a building volume estimation model follows the approach outlined in previous research by our team (Liang et al., 2023c). The process began with segmenting the NTL data of YRD into distinct built-up area (BUA) cells, serving as proxies for the centers of human activity. These BUA cells were then categorized into clusters based on their luminous efficiency, derived from the NTL data. Utilizing this classification, we estimated the building volume within the YRD at the micro-unit scale (i.e., BUA) for the period from 2000 to 2020.

(1) Built-up area cells extraction

The extraction of built-up area cells was accomplished through an analysis of NTL data, employing the watershed analysis technique to divide the urban area into distinct cell units. This method, detailed in Liang et al. (2023c), relies on the principles of luminescence observed in nighttime data to define the cells. Subsequently, these cells were organized into three clusters based on their luminous efficiency, as shown in Table 2, which aligned with our previous research (Liang et al., 2023c), with the validation of coefficients presented in Supplementary Fig. S1.

This classification reflects the variance in luminous efficiency across different urban locations, acknowledging that centers of high human activity, such as commercial areas, exhibit higher luminous efficiency compared to less dense areas like the suburbs. The

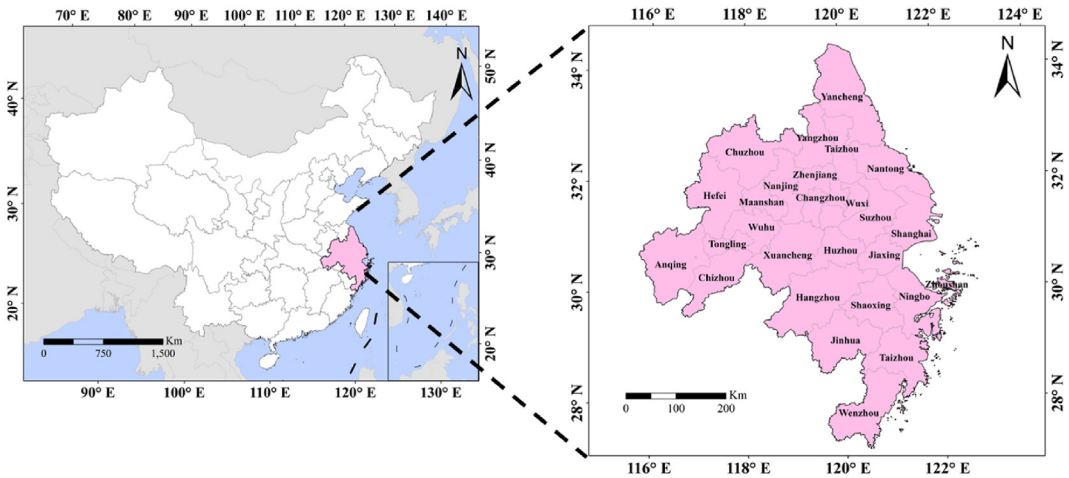


**Fig. 2.** Distribution of YRD and megacities included in the YRD.

**Table 2**
Division of cell cluster.

| Cell cluster | Luminous value range |
|---|---|
| Cluster I | 0–7410 |
| Cluster II | 7410–14347 |
| Cluster III | >14347 |

luminescence efficiency for each BUA was calculated using the formula:

$$LE_i = \frac{N_i}{S_i} \tag{1}$$

where $LE_i$ denotes luminous efficiency of built-up area cell $i$; $N_i$ represents the total nighttime lights luminous of built-up area cell $i$, and $S_i$ indicates the floor area of built-up area cell $i$.

(2) Building volume estimation

The total luminous efficiency of nighttime lights within each BUA was tallied, and the building volume for each BUA was determined using GIS data. By examining the relationship between luminous efficiency and building volume, we quantified their mathematical correlation to develop a model for calculating building volume. Based on the previously calculated luminous efficiency, buildings were categorized into three groups. The criteria for division and the determination of coefficients are referenced from Liang et al. (2023c). The building volume calculation is expressed as:

$$V_{i,j} = \alpha_j \times LE_{i,j} \times S_{i,j} \tag{2}$$

where $V_{i,j}$ represents the building volume of built-up area cell $i$ in cluster $j$, $\alpha_j$ is the coefficient for cluster, $LE_{i,j}$ is the luminous efficiency in cluster $j$; , and $S_{i,j}$ is the area of built-up area cell $i$ in cluster $j$.

### 3.2. Building MS accounting

In this section, we detail the process of accounting for building MS by integrating the derived building volume data with building height and MI values. Our methodology categorizes buildings into residential and non-residential types to estimate the building MS in YRD, based on these classifications. The building MS was calculated using the following formulas:

$$MS = \sum MS_{i,j,k} \tag{3}$$

$$MS_{i,j,k} = MS_{i,j,k}{}' + MS_{i,j,k}{}'' \tag{4}$$

$$MS'_{i,j,k} = \frac{V_{i,j}}{h} \times \beta_j \times MI_k \tag{5}$$

$$MS''_{i,j,k} = \frac{V_{i,j}}{h} \times (1 - \beta_j) \times MI_k \tag{6}$$

where $MS$ represents the total building material stock in YRD;$MS_{i,j,k}$ denotes the material stock of building type $k$ in built-up area cell $i$ within cluster $j$. $MS'_{i,j,k}$ and $MS''_{i,j,k}$ represent the material stock of residential and non-residential buildings, respectively. The variable $V_{i,j}$ represents the building volume of built-up area cell $i$ in cluster $j$, measured in cubic meters ($m^3$), which serves as a foundational metric for building MS calculation. The average floor height, denoted by $h$, is standardized at 3 m based on Chinese standard building requirements, providing a uniform measure for calculating building volumes across different types and clusters. $\beta_j$ represents the proportion of residential buildings in cluster $j$; $MI_k$ represents the amount of construction material k used per square meter in residential buildings or non-residential buildings.

It should be noted that previous studies on urban building dynamics in China, such as those by Li et al. (2023), Liu et al. (2019), Lu et al. (2024), and You et al. (2023), predominantly assessed residential and non-residential building proportions at the city scale. In contrast, our approach delves into a micro-scale analysis, using NTL data segmented into three distinct clusters to differentiate building types within urban areas. This method allows us to provide a granular view of urban structures, essential for assessing the MS and ECE accurately. We applied OpenStreetMap (OSM) data to determine building proportions within each cluster for the year 2020, applying these classifications retrospectively across the study period. This nuanced approach revealed significant variations in building types across clusters: Cluster III, characterized by high luminous efficiency, predominantly includes commercial buildings and thus has a lower proportion of residential structures, whereas Cluster I, with lower luminous efficiency, indicates a higher proportion of residential buildings. These distinctions are further illustrated in Fig. S1, which visually depicts the division of residential and non-residential buildings at a micro-scale. The proportion of residential to non-residential buildings within each cluster, as detailed in Table 3, is

instrumental in differentiating material stocks between building types.

The MI values utilized in our calculations, derived from the comprehensive analysis by Li et al. (2023), are presented in Table 4. This expanded MI dataset encompasses 11 materials, including three metals and eight non-metals, facilitating a more detailed analysis of material use differences. The inclusion of this detailed MI enables us to more accurately account for the building MS, particularly in distinguishing between metallic and non-metallic material use across different building types.

### 3.3. Building ECE accounting

LCA methodology encompasses various stages in the life cycle of construction materials, where "cradle to gate" stage accounts for 62% of the total building ECE across the entire life cycle (Liang et al., 2023a), underscoring the importance of accurately quantifying building ECE during this initial stage. Accordingly, our study zeroes in on the building ECE emitted during the "cradle to gate" stage, utilizing the following formulae to calculate building ECE based on the building MS and EF:

$$ECE = \sum ECE_i \tag{7}$$

$$ECE_i = EF_i \times MS_i \tag{8}$$

where $ECE$ represents the total building embodied carbon emission in YRD; $ECE_i$ denotes the building embodied carbon emission in cell $i$; $EF_i$ is the carbon emission factor associated with each material in cell $i$; $MS_i$ indicates the building material stock in cell $i$.

EF is derived from the Standard for Building Carbon Emission Calculation (Ministry of Housing and Urban-Rural Development of the People's Republic of China, 2019). The specific EF values for various building materials are detailed in Table 5, facilitating an accurate assessment of building ECE based on the composition and quantity of materials used in construction.

### 3.4. Trend analysis method

The Sen's Slope Estimator Test, a robust method for trend analysis introduced by Sen (1968), was utilized in this study to evaluate the growth trends of building ECE across cities within YRD. The slope ($sl$) of building ECE for each city was determined using the following formula:

$$sl = Median\left(\frac{ECE_s - ECE_t}{s - t}\right) \tag{9}$$

where $Median$ represents the median of $sl$ values; $ECE_s$ and $ECE_t$ denote the building ECE for year $s$ and $t$ respectively, with $s > t$. Incorporating a comprehensive time series of building ECE data as input, and setting a 90% confidence level, we meticulously calculated the trend of building ECE changes spanning from 2000 to 2020 through the application of formula (9).

### 3.5. Standard deviational ellipse (SDE) method

This study employed SDE method to measure the development trends of the building MS in YRD. The SDE serves as a pivotal statistical instrument within the realm of multivariate analysis, finding its niche applications predominantly in spatial analysis and ecological studies. It provides a visual depiction of the variability inherent in a dataset through a two-dimensional graphical construct, delineating the standard deviations of individual data points relative to the central mean. The calculating process mainly includes two steps, detailed as follows.

(1) Calculating the mean center of all cells

Then, the average MS value of all cells is calculated as the mean center, utilizing the following formula:

$$\overline{MS} = \frac{1}{n}\sum_{i=1}^{n} MS_i \tag{10}$$

where $\overline{MS}$ represents mean center of MS value of all cells; $n$ is the total number of the cell.

**Table 3**
Proportion of residential and non-residential buildings across the three luminosity-based cell clusters.

| Cell cluster | Residential proportion | Non-residential proportion |
|---|---|---|
| Cluster I | 38.54% | 61.46% |
| Cluster II | 29.87% | 70.13% |
| Cluster III | 22.10% | 77.90% |

Note: Cluster I represents the low luminous value in build-up areas; Cluster II represents the middle luminous value in build-up areas; Cluster III represents the high luminous value in build-up areas.

**Table 4**
Material intensity of for 11 construction materials across residential and non-residential building types derived from Li et al. (2023) (kg/m$^2$).

| Construction material *k* | Residential building | Non-residential building |
|---|---|---|
| Steel | 40 | 80 |
| Copper | 30 | 60 |
| Aluminum | 0.5 | 4 |
| Timber | 27 | 27 |
| Brick | 180 | 234 |
| Gravel | 881 | 750 |
| Sand | 800 | 800 |
| Asphalt | 2 | 2 |
| Lime | 33 | 28 |
| Glass | 2 | 2 |
| Cement | 238 | 418 |
| Total | 2203.5 | 2345 |

**Table 5**
Carbon emission factor for different construction materials (t/t).

| Building material | Steel | Copper | Aluminum | Timber | Brick | Gravel | Sand | Asphalt | Lime | Glass | Cement |
|---|---|---|---|---|---|---|---|---|---|---|---|
| EF | 2140 | 4850 | 15450 | 178 | 295 | 2.18 | 2.51 | 0.51 | 1190 | 1130 | 735 |

(2) Calculating standard deviation

Calculate the covariance matrix central points of each cell, involving the offset of each central point relative to the mean center. Then, we can calculate the standard deviation from the covariance matrix, which represents the degree of concentration of the surface data distribution:

$$C = \frac{1}{n-1}\sum_{i=1}^{n}(MS_i - \overline{MS}) \tag{11}$$

$$\sigma = \sqrt{C} \tag{12}$$

where $\sigma$ is the standard deviation value.

### 3.6. Getis-Ord Gi* statistic method

In this study, we utilized Getis-Ord Gi* statistic method to evaluate the evolution of the building ECE in YRD. The Getis-Ord Gi* statistic is a measure used in spatial analysis to identify clusters of high or low values in a set of geographical data, which is particularly useful for detecting local spatial autocorrelation. The Getis-Ord Gi* statistic is designed to detect clusters of high or low values within spatial data, which can be important in fields such as epidemiology, ecology, and urban planning, versatile and can be applied to various types of spatial data, including point data, areal data, and lattice data. The calculating process mainly includes two steps, detailed as follows.

(1) Calculating local average and local sum

For each cell *i*, calculate the average and sum of the values of all the cells in its neighborhood, and the formula is as follows:

$$ECE_{sumi} = \sum_{r\in D_i} ECE_r \tag{13}$$

$$\overline{ECE_i} = \frac{ECE_{sumi}}{b_i} \tag{14}$$

where $ECE_{sumi}$ represents the sum of the values of all the neighborhood cells in cell *i*; $D_i$ is the neighborhood set; $b_i$ denotes the number of the cells in the neighborhood; $ECE_r$ is the value in the neighborhood cell.

(2) GI* statistic calculating and standardization

For each cell i, the GI* statistic is calculated and standardized with the following formula:

$$GI_i^* = \frac{ECE_i - \overline{ECE_i}}{\sigma_z} \cdot \frac{\sum_{r \in D_i} w_{ir}(ECE_r - \overline{ECE_i})}{\sum_{r \in D_i} w_{ir}} \tag{15}$$

$$GI_{is}^* = \frac{GI_i^*}{\sqrt{E(GI_i^*)^2}} \tag{16}$$

where $GI_i$* denotes GI* statistic of cell $i$; $ECE_i$ represents the ECE value of cell $i$; $\overline{ECE_i}$ denotes the average ECE value of all cells; the $GI_{is}$* is the standardized GI* statistic of cell $i$;

## 4. Study area and data source

### 4.1. Data source

#### 4.1.1. NTL data

So far, two primary sets of NTL data have been widely utilized for urban studies. The initial dataset, Defense Meteorological Satellite Program (DMSP)/Operational Line Scan (OLS) stable NTL data available up to 2012, was marked by a coarse spatial resolution of approximately 1000m, issues of over-saturation, and the absence of on-orbit calibration, limiting its utility for detailed analysis (Letu et al., 2010; Ma et al., 2014; Sutton, 2003). In response to these limitations, National Geophysical Data Center (NGDC) of the National Oceanic and Atmospheric Administration (NOAA) introduced a new generation of NTL data in early 2013 — the Suomi National Polar-orbiting Partnership Visible Infrared Imaging Radiometer Suite (S-NPP VIIRS) NTL composite data. This dataset offers improved spatial resolution of 500 m and resolves the saturation problem inherent in previous datasets (Baugh et al., 2013; Elvidge et al., 2013). To ensure data continuity, Hu et al. (2021) harmonized these two datasets, creating a unified long-term NTL dataset. Utilizing this unified NTL dataset, our study examines the variation in building MS and ECE within YRD from 2000 to 2020.

#### 4.1.2. GIS data

The GIS data employed in this research encompasses two primary sources.

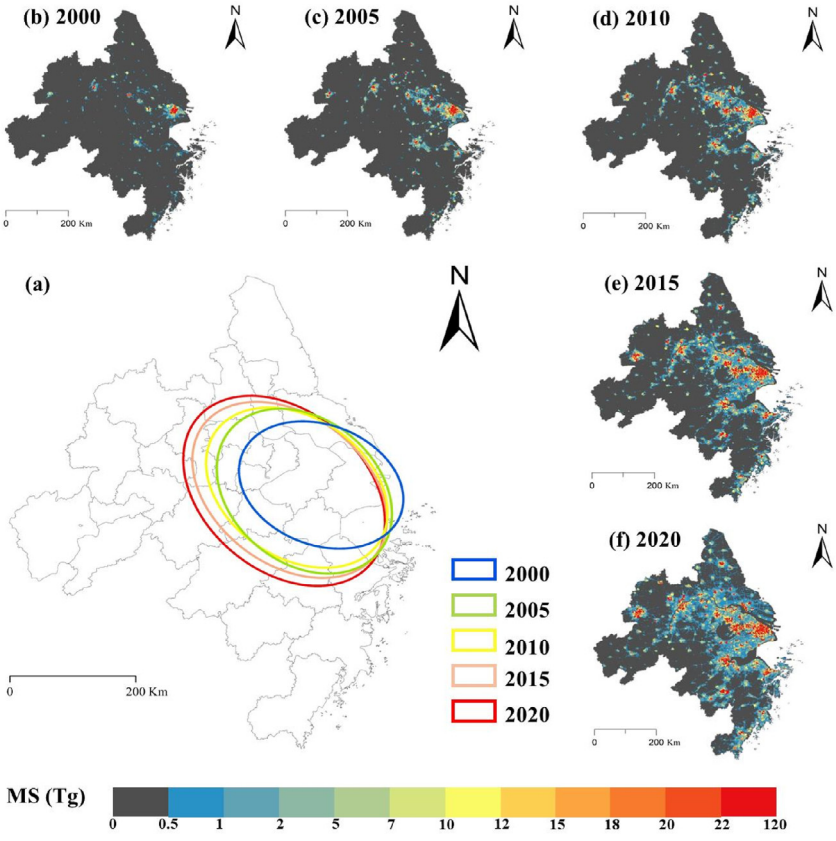


**Fig. 3.** Spatial distribution and development trends of building material stock (MS) in YRD at the micro-unit scale from 2000 to 2020.

(1) **Building Extensive Shape Data**: Acquired from the Resources and Environmental Science and Data Center of the Chinese Academy of Sciences and AutoNavi Navigation Technology Company. This dataset provides essential details (spatial location, floor area, and height) for the majority of urban buildings in 27 megacities within the YRD as of 2020, enabling the generation of building volumes. However, it lacks information on land-use types.

(2) **OpenStreetMap (OSM)**: To complement the first dataset, OSM data was employed to include various land-use types within the YRD in 2020, such as residential and commercial lands. This study utilized OSM to categorize land into residential and non-residential areas, positing that buildings within residential zones are predominantly residential. Together, these datasets facilitated the creation of a comprehensive building extensive shape database, serving as the observational basis for our analysis.

### 4.2. Study area

YRD, an eminent urban agglomeration in Eastern China, encompasses 27 cities, including Shanghai, Hangzhou, and Nanjing (Fig. 2). Distinguished by its economic dynamism, technological innovation, and significant contributions to China's GDP, the YRD is a pivotal region for national urban development. With its dense population, rapid urbanization, and an extensive transportation network, the YRD plays a crucial role in driving economic growth and fostering international trade.

## 5. Results

### 5.1. Temporal-spatial characteristics of building MS in YRD

Fig. 3 shows spatial distribution and pattern of building MS in YRD at the micro-unit scale from 2000 to 2020. Using Standard Deviational Ellipse (SDE) analysis, we observed a significant concentration of development in the eastern coastal regions (Fig. 3(a)). The development trajectory expanded more rapidly along the southeast-northwest axis than the southwest-northeast axis. Over the two decades, the focal areas of MS shifted from major cities like Shanghai and Suzhou to a broader range of cities, including Nanjing and Hangzhou, reflecting wider regional development trends.

Moreover, Fig. 3(b)–(f) presents a detailed visualization of the dynamic changes in building MS within the YRD at the micro-unit scale (i.e., BUA), charted at five-year intervals from 2000 to 2020, with additional year-by-year analysis available in Supplementary Fig. S4. This period saw a remarkable increase in building MS, highlighting the intense urbanization the YRD experienced. Initially, building MS was scattered but gradually coalesced into densely populated areas, particularly in the central, southern, and eastern coastal regions. By 2020, as shown in Fig. 3(e), built-up areas had expanded extensively throughout the YRD. This expansion not only indicates a substantial increase in building MS but also reveals a pattern of urban sprawl extending from coastal regions toward inland areas, reflecting significant urban growth and the evolving landscape of the region.

The temporal variation of MS in residential and non-residential buildings of YRD, as depicted in Fig. 4(a), shows a remarkable increase from 2000 to 2020. Throughout this period, the total building MS surged from 2642.73 Teragrams (Tg) to 37,732.31 Tg, an over fourteenfold increase. Specifically, the MS of residential buildings rose from 713.54 to 10,187.72 Tg, constituting 26.27% of the

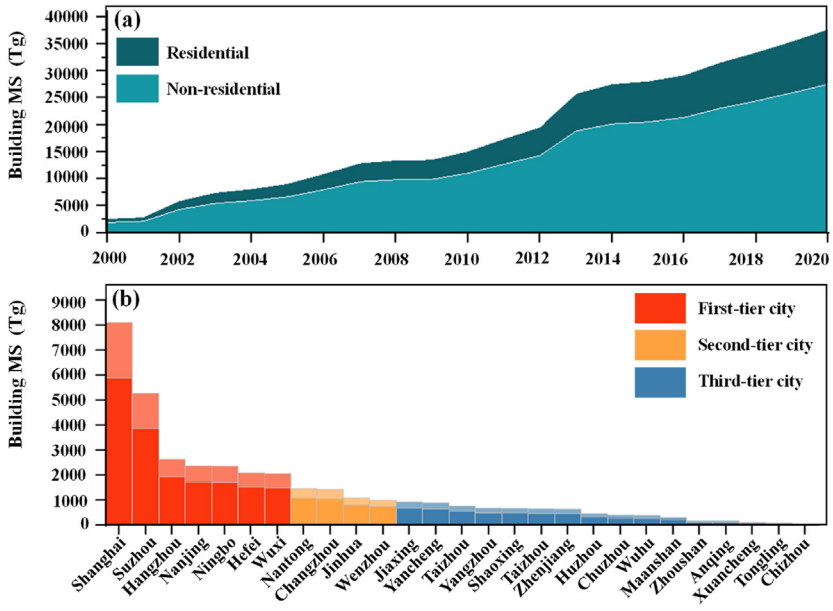


**Fig. 4.** Temporal variation of building material stock (MS) in YRD, 2000–2020: (a) of residential and non-residential building MS, (b) MS distribution across cities in 2020.

total building MS. In contrast, non-residential buildings experienced an increase from 1929.19 Tg to 27,544.58 Tg, representing 73.73% of the total MS.

Fig. 4(b) categorizes the building MS across different cities within YRD in 2020 into three tiers based on their MS: First-tier cities with MS $\geq$ 2000 Tg, Second-tier cities with 1000 Tg $\leq$ MS $<$ 2000 Tg, and Third-tier cities with MS $<$ 1000 Tg. This categorization highlights the spatial disparities in building MS among the YRD cities. Among the seven first tier cities, Shanghai stood out with the highest MS, comprising 21.47% of the YRD's total, reaching 8102.59 Tg—2187.7 Tg in residential and 5914.89 Tg in non-residential buildings. Suzhou, with a total MS of 5292.45 Tg—1428.96 Tg residential and 3863.49 Tg non-residential—was the second highest, accounting for 14.03% of the total. Other first-tier cities, including Hangzhou, Nanjing, Ningbo, Hefei and Wuxi, had their MS in the range of 2000 Tg to 3000 Tg. The MS of second-tier cities (Nantong, Changzhou, Jinhua and Wenzhou) contributed to 13.41% of the YRD's total MS, summing up to 5061.47 Tg—1366.6 Tg residential and 3694.88 Tg non-residential. Meanwhile, the building MS of third-tier cities comprised 20.35% of the total MS in the YRD, with a collective sum of 7676.69 Tg—2072.71 Tg residential and 5603.99 Tg non-residential.

### 5.2. *Temporal-spatial characteristics of building ECE in YRD*

A detailed analysis of building ECE within the YRD from 2000 to 2020 is presented in Fig. 5, employing a micro-unit scale for detailed observation. This period witnessed an extraordinary growth in building ECE, particularly in the central and eastern regions of the YRD, where the total building ECE experienced a fourteenfold increase from 753.19 Tg to 10,736.38 Tg. Such a distribution underscores the rapid and diverse expansion of building ECE across the YRD, with coastal areas notably exhibiting high levels of ECE. Shanghai was at the forefront of this expansion, serving as the epicenter of building ECE with high concentrations spreading from the city's core to surrounding areas. The pattern of spatial expansion varied among cities: cities like Shanghai, Suzhou, Hangzhou, Hefei, and Yancheng showed circular expansion from their urban centers, whereas Nanjing and Wenzhou demonstrated linear growth towards the northeast and southwest, respectively.

We also analyzed the trend variation of ECE in YRD by utilizing Hot Spot Analysis (Fig. 5(b)). This analysis revealed the evolution of ECE distribution from a concentrated single-center pattern in 2000 towards a more dispersed multi-center configuration by 2020. In 2000, the ECE was primarily centered on the eastern coast of the YRD, with Shanghai being the main hotspot. By 2010, there was a notable expansion of the main center, now including Hefei, Nanjing, Suzhou, Shanghai, and Hangzhou. Between 2010 and 2020, the main center continued to grow, and the hotspot region expanded further. Notably, the transformation highlights areas with increasing ECE intensities, particularly in urban centers like Shanghai and Suzhou, which have merged into significant hotspots of carbon emissions.

Further detailed in Fig. 6 is the city-scale spatial and temporal variation of building ECE, underscoring the accelerated growth across the YRD cities from 2000 to 2020. Shanghai maintained a leading position, with its building ECE starting at 509.85 Tg in 2000—then constituting one-third of the YRD's total—and escalating to 2293.70 Tg by 2020, thereby comprising about one-fifth of the total. Suzhou experienced a significant rise in building ECE, from 32.85 Tg to 1502.90 Tg, marking an increase of 4475.04%. Other cities also saw substantial ECE growth, with Hangzhou's ECE up by 2152.88%, Ningbo's by 5072.65%, Nanjing's by 1605.31%, Hefei's by 3779.09%, and Wuxi's by 2858.58%. Fig. 6(f) illustrated the trend magnitude of building ECE in each YRD city, employing Sen's Slope method for analysis. The precise evaluations of these trends, further substantiated by detailed validations, are accessible in Supplementary Fig. S6.

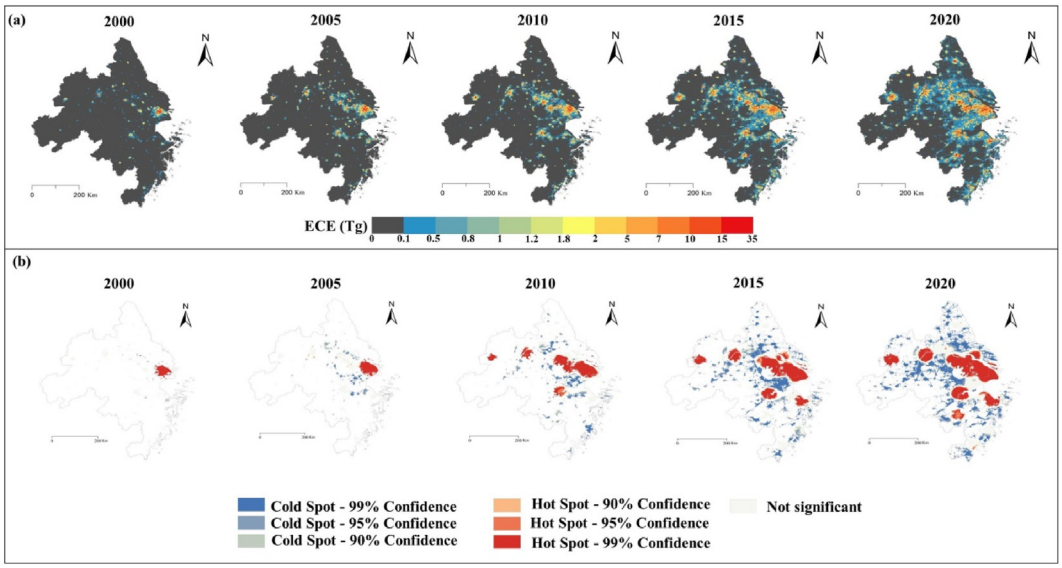


**Fig. 5.** Spatial distribution and evolution of building embodied carbon emission (ECE) in YRD at the micro-unit scale from 2000 to 2020.

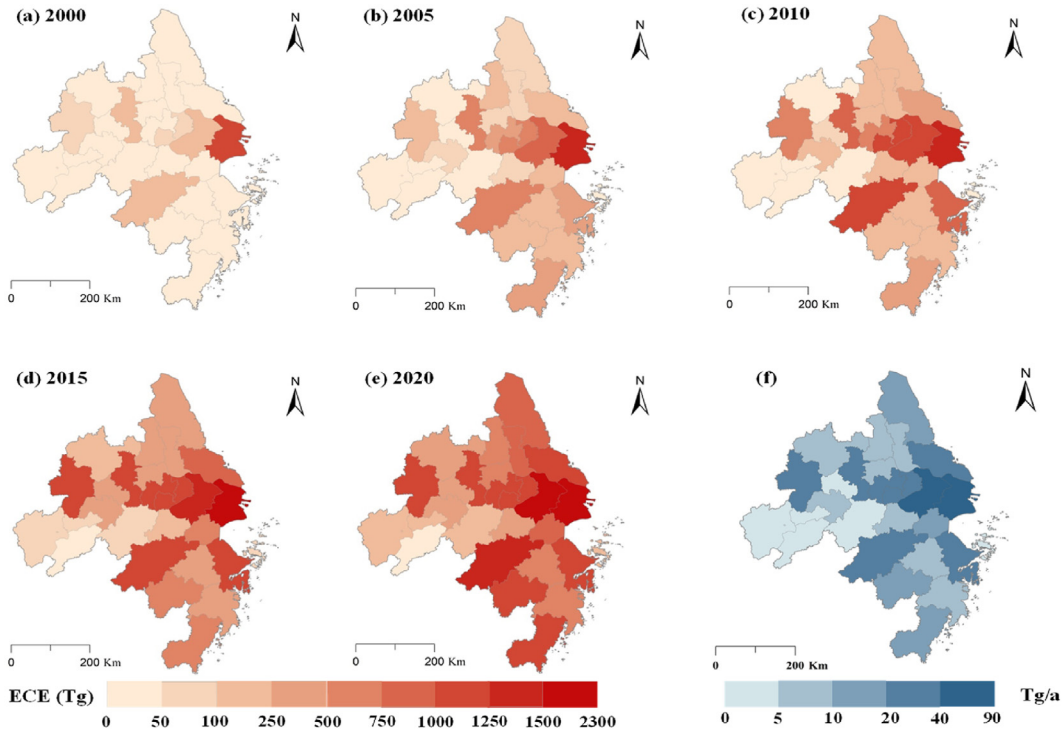


**Fig. 6.** City-scale analysis of building embodied carbon emission (ECE) in YRD, 2000–2020: (a)–(e) ECE distributions, (f) ECE growth trends using Sen's slope method.

The growth trends of building ECE among these cities vary significantly, ranging from 0.64 Teragrams per year (Tg/a) to 85.71 Tg/a. Notably, Shanghai and Suzhou exhibit the most rapid increases in building ECE, with trends recorded at 85.71 Tg/a and 80.14 Tg/a, respectively, significantly outpacing the growth trends observed in other regions of the YRD. Conversely, cities such as Zhoushan, Anqing, Xuancheng, Tongling, and Chizhou are characterized by more modest ECE growth trends, indicating a varied pace of urban

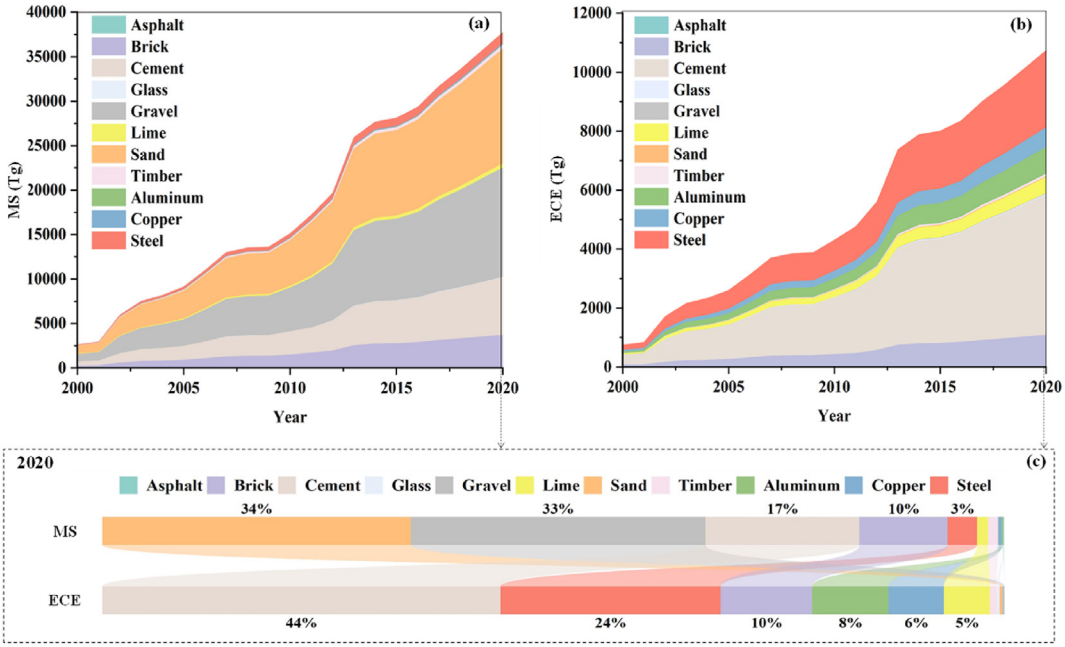


**Fig. 7.** Temporal dynamics of building material stock (MS) and embodied carbon emission (ECE) by materials in YRD, 2000–2020: (a) (b) Yearly trends, (c) Material proportions in MS and ECE in 2020.

development and associated carbon emission increases across the region.

This analysis positions Shanghai as the leading contributor to building ECE in the YRD, with notable increases observed across other cities, particularly Suzhou. The diverse growth patterns across the YRD emphasize the complexity of building ECE expansion, indicating a pressing need for nuanced carbon management and mitigation strategies in this rapidly urbanizing area.

### 5.3. Interactional characteristics of building MS and ECE for construction materials in YRD

Fig. 7 reveals significant variances in the building MS of different construction materials from 2000 to 2020. Sand, gravel, cement, and brick as foundational materials a critical role in the region's construction sector, highlighting their significant contribution to the YRD's building MS expansion. Notably, the building MS of sand and gravel saw the most considerable increases, with sand rising from 903.5 Tg to 12,905.31 Tg (a growth rate of 1328.36%) and gravel from 860.89 Tg to 12,314.08 Tg (1330.39%). Cement and brick also experienced significant expansions, with cement increasing from 453.03 Tg to 6447.12 Tg (1323.11%) and brick from 258.56 Tg to 3686.03 Tg (1325.60%). By 2020, sand and gravel together constituted two-thirds of the total building MS in the YRD, with sand alone representing 34% of the total building MS, followed by gravel (33%), cement (17%), and brick (10%).

Contrasting with the building MS distribution, the building ECE dynamics across various construction materials present a different picture (Fig. 7). Cement, steel, brick and aluminum captured the majority of building ECE, served as the main contributors to the urban environmental issues. In stark contrast, sand and gravel, despite their significant building MS, contributed minimally to building ECE growth. Cement led the increase in building ECE, soaring from 332.98 Tg to 4738.63 Tg (a growth rate of 1323.10%), surpassing all other materials. Steel, brick, and aluminum also saw substantial increases in building ECE, with steel rising from 184.29 Tg to 2621.02 Tg (1322.23%), brick from 76.28 Tg to 1087.38 Tg (1325%), and aluminum from 64.07 Tg to 908.04 Tg (1317.26%), while sand's increased from 2.27 Tg to 32.39 Tg and gravel's from 1.88 Tg to 26.84 Tg. In 2020, cement's building ECE constituted 44% of the total, nearly half, while steel (24%), brick (10%), and aluminum (8%) followed, with sand and gravel accounting for merely 0.3% and 0.25%, respectively.

The divergence between building MS and ECE for different materials highlights a clear trend toward sustainable development in the YRD. The disparity underscores the evolving prioritization of materials that contribute less to carbon emissions, reflecting a strategic shift in the construction sector. As urbanization in the YRD progresses, the focus on materials with lower carbon footprints becomes increasingly crucial, underscoring the importance of sustainable practices in fostering environmentally conscious urban growth.

The MS and ECE within residential and non-residential buildings have shown substantial increases from 2000 to 2020 (as depicted in Fig. 8). Sand, gravel, cement, and brick constitute the majority of MS across both building types. However, the ECE patterns differ notably: steel and cement are predominant contributors to ECE in both building types, while aluminum and brick also significantly impact the ECE metrics in these categories. These findings underscore the material-specific environmental impacts and are critical for

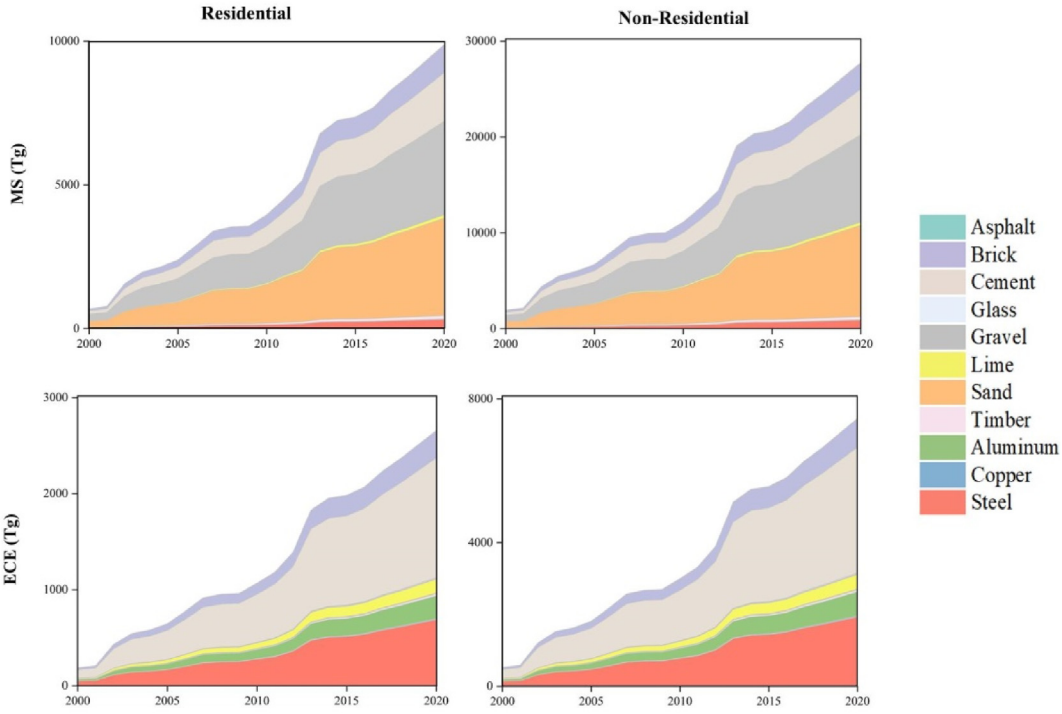


**Fig. 8.** Temporal variation of building material stock (MS) and embodied carbon emission (ECE) for different construction materials in residential and non-residential buildings in YRD, 2000–2020.

urban sustainability planning.

Fig. 9 delineates the disparities in building MS and ECE among key metallic materials—steel, copper, and aluminum—from 2000 to 2020. Throughout this period, all three metals experienced a rapid increase in both building MS and ECE, with growth rates closely aligned: steel's building MS and ECE surged by 1322% and 1321%, copper's by 1361% and 1362%, and aluminum's by 1319% and 1317%. Despite similar growth rates, the total volume of these metals varied significantly. From 2000 to 2020, steel's building MS increased from 86.12 Tg to 1224.77 Tg, copper's from 9.32 Tg to 136.24 Tg, aluminum's from 4.15 Tg to 58.77 Tg. While in terms of building ECE, steel's increased from 184.29 Tg to 2621.02 Tg, copper's from 45.18 Tg to 660.78 Tg, and aluminum's from 64.07 Tg to 908.04 Tg.

However, the distribution of building ECE across these materials depicted huge differences compared with that of building MS. despite the lower building MS contributions of metallic materials, such as copper and aluminum, saw their building ECE proportions increase significantly, and conversely, steel captured significant share in both building MS and ECE among metallic materials, but the proportion of building ECE markedly decreased in comparison to its building MS share. A comparison of the building MS and ECE proportions in 2020 reveals this stark contrast: the metallic materials comprised only 3.8% of the total building MS, they contributed to 36.9% of the building ECE. Steel, as the predominant metal used in urban construction within the YRD, made up 3.2% of building MS in all construction materials, and 86.26% in metallic materials, while its building ECE accounted for 24% in all construction materials, and 62.56% in metallic materials. Copper and aluminum contributed much smaller shares, at 0.4% and 0.2% in all construction materials, and 9.60% and 4.14% in metallic materials respectively. And in terms of building ECE, copper and aluminum accounted for 0.6% in all construction materials, and 5.8% and 8% in metallic materials.

These results underscore that while metallic materials may constitute a minor portion of the construction materials used, they can have a disproportionately large environmental impact. The observed trend, especially the sharp increase in building ECE contributions from copper and aluminum, highlights the need for careful consideration of material selection in urban building construction to mitigate environmental impacts in the YRD.

## 6. Discussion

### 6.1. Comparison with previous research

The MS results from this study were compared with those from Liang et al. (2023c), Sun et al. (2023), Li et al. (2023) and Huang et al. (2023). As depicted in Fig. 10 and Supplementary Tables S1 and S2, the scale and rankings of MS across various cities were generally consistent among the studies, with no significant discrepancies in order or magnitude. This consistency supports the reliability of our findings. Despite this overall alignment, notable variances emerged, warranting a deeper exploration. These discrepancies can be attributed primarily to two factors: the distinct nature of source data utilized and the differential scope of study objects.

Our methodology for estimating MS diverges notably from Huang et al. (2023)'s, Sun et al. (2023)'s and Li et al. (2023)'s approach, primarily through our reliance on Nighttime Light (NTL) data as opposed to their use of multisource big geodata and inventory data. The intensity of NTL, inherently linked to human activities, introduces unique variances in MS estimations. For instance, under-developed suburban areas—such as counties like Qixia and Gaochun in Nanjing, and Tonglu and Jiande in Hangzhou—tend to exhibit lower NTL luminance due to high housing vacancy rates, leading to an underestimation of MS in these regions. Conversely, densely populated urban centers like Shanghai and Suzhou, which attract significant population influxes, demonstrate elevated NTL luminance, potentially resulting in overestimations of MS. Unlike our study, Huang et al. (2023)'s model on MS accounting primarily relies on multisource big geodata accessible within urban built-up areas, thus it remains unaffected by the differences in regional economic activity intensities. However, due to the limited availability of big data in suburban areas, it cannot cover as many buildings within the urban administrative boundaries as included in our study. Furthermore, our classification of buildings into residential and non-residential types contrasts with

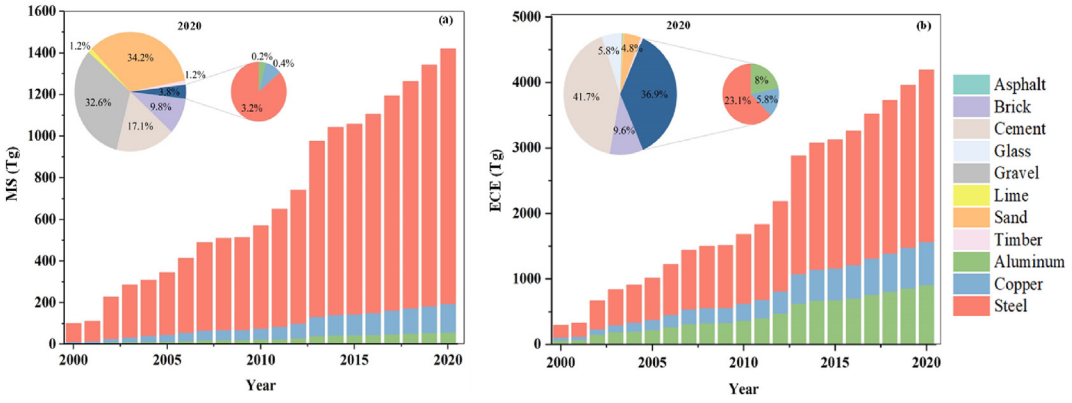


**Fig. 9.** Trends in metallic materials in building construction within the YRD, 2000–2020: (a) (b) Building material stock (MS) and embodied carbon emission (ECE) variations and proportions by materials in 2020, respectively.

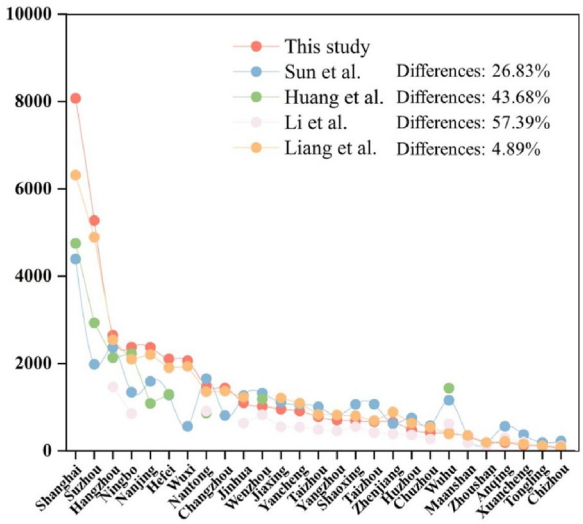


**Fig. 10.** Comparison of estimated material stock (MS).

Huang et al. (2023)'s more granular categorization, which includes 12 types of non-residential buildings alongside residential ones. This difference in building classification, combined with our comprehensive inclusion of MS across the entire urban administrative boundary, likely contributes to our MS estimations being somewhat higher than those reported by Huang et al. (2023).

While this study has not directly compared the ECE results with those of other research due to the absence of comparable "cradle to gate" stage ECE data for other cities, the credibility of our MS findings lends indirect support to the reliability of our ECE estimations. Since ECE at the "cradle to gate" stage is inherently a function of MS combined with emission factors, the robustness of our MS estimations indirectly supports the reliability of our ECE calculations. Furthermore, our approach utilizes a more detailed inventory, categorizing construction materials into 11 distinct types, including three metallic and eight non-metallic materials. This granularity not only enhances the precision of MS and ECE accounting but also represents an innovation in the methodology for urban-scale construction MS accounting. The significant variation in the performance of metallic materials in terms of MS and ECE prompted a focused comparative analysis, distinguishing the MS and ECE contributions of these materials. By dissecting the usage and energy consumption profiles of various construction materials with such specificity, our study is uniquely positioned to offer more scientifically grounded recommendations for the sustainable urban development of the YRD.

### 6.2. *Development pattern of cities in YRD and implications*

Our analysis of building ECE in the YRD from 2000 to 2020 offers insights into the environmental impact of construction materials and reflects the developmental trajectory of cities within the region. The rapid growth in building ECE, primarily concentrated in urban agglomerations, signifies a direct correlation with building MS, underscoring urbanization's significant resource consumption and

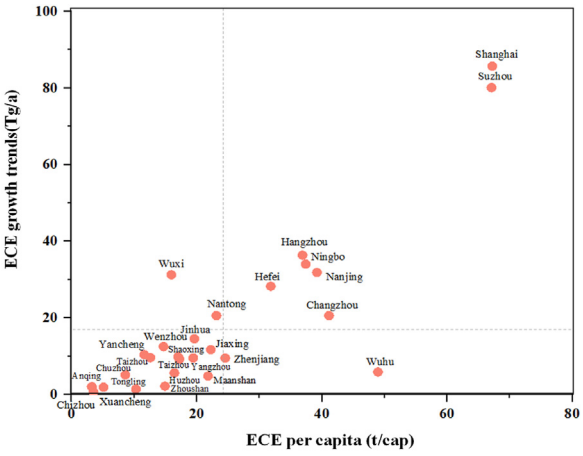


**Fig. 11.** Comparison between average building embodied carbon emission (ECE) per capita and the ECE growth trends across YRD megacities, 2000–2020.

greenhouse gas emissions. Sustainable management of urban building systems emerges as a pivotal strategy for mitigating global resource depletion and environmental impacts. By examining the spatial and temporal characteristics of building ECE, we have outlined the material and energy consumption profiles of the YRD over the past two decades, revealing differences in building ECE among various cities.

To propose actionable strategies for urban sustainable development, we evaluated the average per capita building ECE during 2000–2020 alongside the ECE growth trends, as illustrated in Fig. 11. This assessment enabled categorization of cities into four distinct types based on the mean value of per capita building ECE and growth trends: H-H (high ECE per capita and growth trend), H-L (high ECE, low growth), L-H (low ECE, high growth), and L-L (low ECE and growth). According to Table 6, the LL category includes the majority, with 16 cities representing 59.26% of the YRD's total, followed by the H-H category with 7 cities or 25.93%. Both the H-L and L-H categories comprise 2 cities each, accounting for 7.41% of the total cities in the YRD. This classification reveals the disparities in building ECE and its growth trends, which could hinder sustainable economic development and the achievement of "dual carbon" goals by 2060. Accordingly, our recommendations for YRD's future development focus on tailored strategies for each city type.

(1) H-H Cities: These cities have experienced extensive development since 1978 and have become megacities and key economic and political centers in China. Their favorable locations have attracted large populations, capital, and material resources, leading to substantial material consumption and making them major contributors to building ECE. Moving forward, H-H cities should prioritize high-quality growth by improving resource utilization efficiency amid their significant urban size and rapid expansion. This strategy aims not only to mitigate the environmental impacts of ECE but also to bolster the development of neighboring cities with slower growth, thereby playing a vital role in regional advancement.
(2) H-L Cities: Having built a strong urban foundation during the early stages of China's reform, H-L cities have seen slower growth over the past two decades, reducing their ability to attract external resources. It is advisable for these cities to leverage their existing infrastructure to accelerate urbanization while effectively managing building ECE. Emphasizing the improvement of construction material recovery rates and implementing policies to regulate ECE will be critical. Such strategies are essential for elevating the quality of urban development in H-L cities, ensuring a balance between urban expansion and environmental sustainability.
(3) L-H Cities: Initially, L-H cities did not experience rapid development. However, the onset of economic globalization and China's economic ascent has ushered these cities into a phase of swift urbanization and economic growth. It is important for these cities to continue developing thoughtfully, ensuring that urban expansion is managed sustainably. Adopting environmentally friendly construction materials during this process is crucial to prevent long-term environmental damage. This strategy aims to balance urban growth with ecological preservation, promoting sustainable urban expansion.
(4) L-L Cities: Compared to other areas in the YRD, L-L cities lack significant competitive advantages, limiting their urban scale and growth potential, and thus minimizing their environmental impact. The inherent limitations of these cities hinder substantial progress within a short timeframe if relying solely on their existing attributes. To foster growth, these cities should focus on enhancing connections with the region's megacities and implement incentive policies to attract a variety of resources. This strategy is designed to leverage regional strengths, promoting development through collaboration and synergy with larger urban centers.

### 6.3. The interrelation between MS and ECE

Rapid urbanization has fueled growth in the construction industry, leading to a substantial increase in MS. As urban infrastructures expand, the demand for construction materials rises, directly influencing MS levels. This growth in MS is inherently linked to significant energy consumption and raw material usage during construction, which are primary sources of carbon emissions. Thus, the correlation between MS magnitudes and the construction sector's carbon footprint is evident.

ECE are most significant during the early life cycle stages of building materials, particularly from "cradle to gate." Emissions during this stage are crucial in determining the overall carbon footprint of a building's life cycle. Different materials have varying carbon emission factors; for example, producing steel and concrete involves high energy use and emissions, while wood and other renewable materials generally have lower carbon impacts.

To address the urgent need for sustainable urban development, future strategies are likely to focus on reducing ECE and improving building energy efficiency. This emphasis will influence material selection, architectural design, and broader urban planning practices. Policies and regulations can play a pivotal role by promoting the use of low-carbon materials and advocating for greener construction practices. Such measures will help lower ECE and alter the material composition of urban environments.

### 6.4. Limitations and prospects

Although this study provides significant insights into the dynamics of building MS and ECE within the YRD, it has certain limitations. The reliance on OSM data for categorizing buildings into residential and non-residential types restricts access to detailed attribute information, such as the year of construction, floor heights, renovation statuses, and the nuanced classification of non-residential buildings. Furthermore, the material intensity and carbon emission factors used are based on current estimates, which may change with technological advancements, potentially affecting the accuracy of MS and ECE calculations.

To enhance the robustness of future studies, it will be essential to incorporate historical data on material intensity and carbon emission factors for various building materials. This inclusion will ensure temporal accuracy in MS and ECE calculations for longitudinal

**Table 6**
Classification of cities in the YRD based on average building embodied carbon emission (ECE) per capita and the ECE growth trends.

| City type | Cities |
|---|---|
| H-H | Shanghai, Suzhou, Hangzhou, Ningbo, Nanjing, Hefei, Changzhou |
| H-L | Wuhu, Zhenjiang |
| L-H | Wuxi, Nantong |
| L-L | Anqing, Chizhou, Chuzhou, Huzhou, Jinhua, Jiaxing, Maanshan, Shaoxing, Taizhou, Taizhou, Tongling, Wenzhou, Xuancheng, Yancheng, Yangzhou, Zhoushan |

analyses. Moreover, the lack of extensive time-series data on construction and demolition timelines has confined our analysis to the "cradle-to-gate" lifecycle stage, excluding the full lifecycle considerations of building materials. Conducting comprehensive LCA of building ECE in future research will provide a more holistic perspective on the environmental impacts of urban development. Addressing these limitations will significantly refine our understanding of sustainable urbanization and contribute to developing more effective strategies for managing urban growth and mitigating its environmental implications.

Furthermore, this study has primarily focused on MS and ECE without exploring their deeper connections to broader socioeconomic factors such as economic development levels, population density, and technological advancements. Future research should aim to include these variables, employing advanced statistical methods to examine their influence on urban sustainability.

## 7. Conclusion

In light of global warming and significant environmental pollution, it is crucial to explore the spatial dynamics of building MS and ECE to promote sustainable development and achieve carbon neutrality. This study introduces a bottom-up accounting method based on NTL data to estimate and spatially map urban building MS and ECE at the micro-unit scale in the Yangtze River Delta (YRD) from 2000 to 2020, focusing on the "cradle to gate" stage. By examining the temporal variations of different construction materials, we offer strategic insights tailored to cities with diverse developmental patterns. Our key findings are.

(1) The YRD experienced a substantial increase in total building MS from 2000 to 2020, with a notable expansion in both residential and non-residential sectors. The spatial distribution of building MS was concentrated mainly in the central and eastern regions, with Shanghai and Suzhou experiencing the most pronounced growth.
(2) Building ECE also saw a dramatic rise during the same period, predominantly in the coastal areas, highlighting the critical roles of Shanghai, Suzhou, Nanjing, and Hangzhou., revealing the interconnected growth across these urban centers.
(3) While sand, gravel, brick, and cement constituted the majority of the YRD's building MS, cement, steel, brick, and aluminum were predominant in driving the increase in building ECE. Despite lower volumes, copper and aluminum demonstrated substantial environmental impacts through their ECE contributions.
(4) The categorization of cities into four distinct types (H-H, H-L, L-H, L-L) based on their building ECE per capita and growth trends highlighted the diverse urban development and environmental impacts across the region. This classification underscores the need for customized urban planning and policy strategies to effectively address the distinct challenges and leverage the opportunities of each city type, promoting sustainable development and carbon emission reduction.

In conclusion, this study provides a comprehensive long-term dataset of building MS and ECE from the "cradle to gate" stage, and marks a substantial step forward in understanding the complex dynamics of building MS and ECE within the YRD. However, we acknowledge certain limitations, such as the reliance on OSM data and the use of current estimates for MI and EF, which may affect the accuracy of our findings over time. Future research should aim to integrate historical data and consider the full life cycle of building materials to enhance the precision of MS and ECE assessments. By extending our analytical framework to encompass comprehensive LCA and addressing the noted limitations, subsequent studies can offer deeper insights into the environmental impacts of urbanization. This progression in research methodology will not only refine our understanding of sustainable urban development but also support the development of nuanced, effective strategies for urban growth management and carbon mitigation in YRD. Our work lays the groundwork for these endeavors, pointing towards a future where urban planning and environmental policy are informed by detailed, longitudinal analyses of building materials and their carbon footprints.

## CRediT authorship contribution statement

**Hanwei Liang:** Writing – review & editing, Writing – original draft, Supervision, Methodology. **Baizhe Zhang:** Writing – original draft, Methodology, Investigation, Formal analysis, Data curation. **Xin Bian:** Writing – review & editing, Methodology. **Jieling Shen:** Writing – review & editing. **Yuxuan Wang:** Writing – review & editing. **Liang Dong:** Writing – review & editing, Supervision, Resources, Methodology, Conceptualization.

## Declaration of competing interest

The authors declare that they have no known competing financial interests or personal relationships that could have appeared to influence the work reported in this paper.

## Acknowledgements

This study is funded by National Natural Science Foundation of China (No. 42001240), Funds for International Cooperation and Exchange of the National Natural Science Foundation of China (No. 42161144003), National College Students' Innovation and Entrepreneurship Training Program, China (202410300041Z, 202410300094Z) and National Natural Science Foundation, China (NSFC), the Dutch Research Council (NWO) (NSFC-NWO, NSFC: 72061137071; NWO: 482.19.608), and the Postgraduate Research & Practice Innovation Program of Jiangsu Province (KYCX24_1409).

## Appendix A. Supplementary data

Supplementary data to this article can be found online at https://doi.org/10.1016/j.jum.2024.10.004.

## References

Acquaye, A., Duffy, A., & Basu, B. (2011). Embodied emissions abatement—a policy assessment using stochastic analysis. *Energy Policy, 39*(1), 429–441.
An, J., Huang, Y., Huang, C., Wang, X., Yan, R., Wang, Q., Wang, H., Jing, S.a., Zhang, Y., & Liu, Y. (2021). Emission inventory of air pollutants and chemical speciation for specific anthropogenic sources based on local measurements in the Yangtze River Delta region, China. *Atmospheric Chemistry and Physics, 21*(3), 2003–2025.
Augiseau, V., & Barles, S. (2017). Studying construction materials flows and stock: A review. *Resources, Conservation and Recycling, 123*, 153–164.
Bai, X. (2016). Eight energy and material flow characteristics of urban ecosystems. *Ambio, 45*(7), 819–830.
Bai, X., Dawson, R. J., Ürge-Vorsatz, D., Delgado, G. C., Salisu Barau, A., Dhakal, S., Dodman, D., Leonardsen, L., Masson-Delmotte, V., & Roberts, D. C. (2018). Six research priorities for cities and climate change. *Nature, 555*(7694), 23–25.
Bai, J., & Qu, J. (2021). Investigating the spatiotemporal variability and driving factors of China's building embodied carbon emissions. *Environmental Science and Pollution Research, 28*, 19186–19201.
Baugh, K., Hsu, F.-C., Elvidge, C. D., & Zhizhin, M. (2013). Nighttime lights compositing using the VIIRS day-night band: Preliminary results. *Proceedings of the Asia-Pacific Advanced Network, 35*(0), 70–86.
Biswas, W. K. (2014). Carbon footprint and embodied energy consumption assessment of building construction works in Western Australia. *International Journal of Sustainable Built Environment, 3*(2), 179–186.
Cabeza, L. F., Rincón, L., Vilariño, V., Pérez, G., & Castell, A. (2014). Life cycle assessment (LCA) and life cycle energy analysis (lcea) of buildings and the building sector: A review. *Renewable and Sustainable Energy Reviews, 29*, 394–416.
Chen, C., Luo, Y., Zou, H., & Huang, J. (2023). Understanding the driving factors and finding the pathway to mitigating carbon emissions in China's Yangtze River Delta region. *Energy, 278*, Article 127897.
Chen, W., Yang, S., Zhang, X., Jordan, N. D., & Huang, J. (2022). Embodied energy and carbon emissions of building materials in China. *Building and Environment, 207*, Article 108434.
Chen, Z., Yu, B., Song, W., Liu, H., Wu, Q., Shi, K., & Wu, J. (2017). A new approach for detecting urban centers and their spatial structure with nighttime light remote sensing. *IEEE Transactions on Geoscience and Remote Sensing, 55*(11), 6305–6319.
Cheng, L., Zhang, T., Chen, L., Li, L., Wang, S., Hu, S., Yuan, L., Wang, J., & Wen, M. (2020). Investigating the impacts of urbanization on PM2. 5 pollution in the Yangtze River Delta of China: A spatial panel data approach. *Atmosphere, 11*(10), 1058.
Cui, S., Zhang, Y., Zhou, J., Lin, J., & Liu, Y. (2011). Research methods and prospects of urban building metabolism. *Ecological Science, 30*(3), 359–367.
Elvidge, C. D., Baugh, K., Zhizhin, M., Hsu, F. C., & Ghosh, T. (2017). VIIRS night-time lights. *International Journal of Remote Sensing, 38*(21), 5860–5879.
Elvidge, C. D., Zhizhin, M., Hsu, F. C., & Baugh, K. (2013). What is so great about nighttime VIIRS data for the detection and characterization of combustion sources. *Proceedings of the Asia-Pacific Advanced Network, 35*(0), 33.
Felicioni, L., Gaspari, J., Veselka, J., & Malík, Z. (2023). A comparative cradle-to-grave life cycle approach for addressing construction design choices: An applicative case study for a residential tower in Aalborg, Denmark. *Energy and Buildings, 298*, Article 113557.
Finnveden, G., Hauschild, M. Z., Ekvall, T., Guinée, J., Heijungs, R., Hellweg, S., Koehler, A., Pennington, D., & Suh, S. (2009). Recent developments in life cycle assessment. *Journal of Environmental Management, 91*(1), 1–21.
Gandy, M. (2004). Rethinking urban metabolism: Water, space and the modern city. *City, 8*(3), 363–379.
Giesekam, J., Barrett, J., Taylor, P., & Owen, A. (2014). The greenhouse gas emissions and mitigation options for materials used in UK construction. *Energy and Buildings, 78*, 202–214.
González, M. J., & Navarro, J. G. (2006). Assessment of the decrease of CO2 emissions in the construction field through the selection of materials: Practical case study of three houses of low environmental impact. *Building and Environment, 41*(7), 902–909.
Gu, C., Hu, L., Zhang, X., Wang, X., & Guo, J. (2011). Climate change and urbanization in the Yangtze River Delta. *Habitat International, 35*(4), 544–552.
Häfliger, I.-F., John, V., Passer, A., Lasvaux, S., Hoxha, E., Saade, M. R. M., & Habert, G. (2017). Buildings environmental impacts' sensitivity related to LCA modelling choices of construction materials. *Journal of Cleaner Production, 156*, 805–816.
Haberl, H., Wiedenhofer, D., Schug, F., Frantz, D., Virág, D., Plutzar, C., Gruhler, K., Lederer, J., Schiller, G., & Fishman, T. (2021). High-resolution maps of material stocks in buildings and infrastructures in Austria and Germany. *Environmental Science and Technology, 55*(5), 3368–3379.
Hammond, G. P., & Jones, C. I. (2008). Embodied energy and carbon in construction materials. *Proceedings of the institution of civil engineers-energy, 161*(2), 87–98.
Han, L., Xu, Y., Lei, C., Yang, L., Deng, X., Hu, C., & Xu, G. (2016). Degrading river network due to urbanization in Yangtze River Delta. *Journal of Geographical Sciences, 26*, 694–706.
Hattori, R., Horie, S., Hsu, F.-C., Elvidge, C. D., & Matsuno, Y. (2014). Estimation of in-use steel stock for civil engineering and building using nighttime light images. *Resources, Conservation and Recycling, 83*, 1–5.
Heisel, F., McGranahan, J., Ferdinando, J., & Dogan, T. (2022). High-resolution combined building stock and building energy modeling to evaluate whole-life carbon emissions and saving potentials at the building and urban scale. *Resources, Conservation and Recycling, 177*, Article 106000.
Hsu, F.-C., Elvidge, C. D., & Matsuno, Y. (2013). Exploring and estimating in-use steel stocks in civil engineering and buildings from night-time lights. *International Journal of Remote Sensing, 34*(2), 490–504.
Hu, M. (2023). A look at residential building stock in the United States-mapping life cycle embodied carbon emissions and other environmental impact. *Sustainable Cities and Society, 89*, Article 104333.

Hu, Y., Chen, J., Cao, X., Chen, X., Cui, X., & Gan, L. (2021). Correcting the saturation effect in dmsp/ols stable nighttime light products based on radiance-calibrated data. *IEEE Transactions on Geoscience and Remote Sensing, 60*, 1–11.
Huang, Z., Bao, Y., Mao, R., Wang, H., Yin, G., Wan, L., … Liu, Q. (2023). Big geodata reveals spatial patterns of built environment stocks across and within cities in China. *Engineering, 34*, 143–153.
Huang, B., Chen, Y., McDowall, W., Türkeli, S., Bleischwitz, R., & Geng, Y. (2019). Embodied GHG emissions of building materials in Shanghai. *Journal of Cleaner Production, 210*, 777–785.
Iso-Norm, I. (2006). *Environmental management—life cycle assessment—principles and framework ISO 14040: 2006*. Geneva, Switzerland: ISO.
Kamali, M., Hewage, K., & Sadiq, R. (2019). Conventional versus modular construction methods: A comparative cradle-to-gate LCA for residential buildings. *Energy and Buildings, 204*, Article 109479.
Kang, G., Kim, T., Kim, Y.-W., Cho, H., & Kang, K.-I. (2015). Statistical analysis of embodied carbon emission for building construction. *Energy and Buildings, 105*, 326–333.
Kaoula, D., & Bouchair, A. (2018). Evaluation of environmental impacts of hotel buildings having different envelopes using a life cycle analysis approach. *Indoor and Built Environment, 27*(4), 561–580.
Kaoula, D., & Bouchair, A. (2020). Identification of the best material-energy-climate compatibility for five ecological houses and the contribution of their impact sources to the overall balance. *Sustainable Cities and Society, 52*, Article 101781.
Kennedy, C., Cuddihy, J., & Engel-Yan, J. (2007). The changing metabolism of cities. *Journal of Industrial Ecology, 11*(2), 43–59.
Kennedy, C., Pincetl, S., & Bunje, P. (2011). The study of urban metabolism and its applications to urban planning and design. *Environmental Pollution, 159*(8–9), 1965–1973.
Krausmann, F., Gingrich, S., Eisenmenger, N., Erb, K.-H., Haberl, H., & Fischer-Kowalski, M. (2009). Growth in global materials use, GDP and population during the 20th century. *Ecological Economics, 68*(10), 2696–2705.
Lavagna, M., Baldassarri, C., Campioli, A., Giorgi, S., Dalla Valle, A., Castellani, V., & Sala, S. (2018). Benchmarks for environmental impact of housing in Europe: Definition of archetypes and LCA of the residential building stock. *Building and Environment, 145*, 260–275.
Lehmann, S. (2011). Optimizing urban material flows and waste streams in urban development through principles of zero waste and sustainable consumption. *Sustainability, 3*(1), 155–183.
Letu, H., Hara, M., Yagi, H., Naoki, K., Tana, G., Nishio, F., & Shuhei, O. (2010). Estimating energy consumption from night-time DMPS/OLS imagery after correcting for saturation effects. *International Journal of Remote Sensing, 31*(16), 4443–4458.
Li, X., Song, L., Liu, Q., Ouyang, X., Mao, T., Lu, H., Liu, L., Liu, X., Chen, W., & Liu, G. (2023). Product, building, and infrastructure material stocks dataset for 337 Chinese cities between 1978 and 2020. *Scientific Data, 10*(1), 228.
Liang, H., Bian, X., & Dong, L. (2023a). Towards net zero carbon buildings: Accounting the building embodied carbon and life cycle-based policy design for Greater Bay Area, China. *Geoscience Frontiers*, Article 101760.
Liang, H., Bian, X., & Dong, L. (2023b). Towards net zero carbon buildings: Accounting the building embodied carbon and life cycle-based policy design for Greater Bay Area, China. *Geoscience Frontiers*, Article 101760.
Liang, H., Bian, X., Dong, L., Shen, W., Chen, S. S., & Wang, Q. (2023c). Mapping the evolution of building material stocks in three eastern coastal urban agglomerations of China. *Resources, Conservation and Recycling, 188*, Article 106651.
Liang, H., Dong, L., Tanikawa, H., Zhang, N., Gao, Z., & Luo, X. (2017). Feasibility of a new-generation nighttime light data for estimating in-use steel stock of buildings and civil engineering infrastructures. *Resources, Conservation and Recycling, 123*, 11–23.
Liang, H., Tanikawa, H., Matsuno, Y., & Dong, L. (2014). Modeling in-use steel stock in China's buildings and civil engineering infrastructure using time-series of DMSP/OLS nighttime lights. *Remote Sensing, 6*(6), 4780–4800.
Liu, T., Zhao, R., Xie, Z., Xiao, L., Chen, A., Feng, W., You, Z., Feng, M., & Li, R. (2023). Carbon emissions from accumulated stock of building materials in China. *Building and Environment, 240*, Article 110451.
Müller, D. B. (2006). Stock dynamics for forecasting material flows—case study for housing in The Netherlands. *Ecological Economics, 59*(1), 142–156.
Müller, D. B., Liu, G., Løvik, A. N., Modaresi, R., Pauliuk, S., Steinhoff, F. S., & Brattebø, H. (2013). Carbon emissions of infrastructure development. *Environmental Science and Technology, 47*(20), 11739–11746.
Ma, L., Wu, J., Li, W., Peng, J., & Liu, H. (2014). Evaluating saturation correction methods for DMSP/OLS nighttime light data: A case study from China's cities. *Remote Sensing, 6*(10), 9853–9872.
Mao, R., Bao, Y., Huang, Z., Liu, Q., & Liu, G. (2020). High-resolution mapping of the urban built environment stocks in Beijing. *Environmental Science and Technology, 54*(9), 5345–5355.
Moncaster, A., & Symons, K. (2013). A method and tool for 'cradle to grave'embodied carbon and energy impacts of UK buildings in compliance with the new TC350 standards. *Energy and Buildings, 66*, 514–523.
Niza, S., Rosado, L., & Ferrao, P. (2009). Urban metabolism: Methodological advances in urban material flow accounting based on the Lisbon case study. *Journal of Industrial Ecology, 13*(3), 384–405.
Pan, D., Yu, X., & Zhou, Y. (2023). Cradle-to-grave lifecycle carbon footprint analysis and frontier decarbonization pathways of district buildings in subtropical Guangzhou, China. *Journal of Cleaner Production, 416*, Article 137921.
Pandit, A., Minné, E. A., Li, F., Brown, H., Jeong, H., James, J.-A. C., Newell, J. P., Weissburg, M., Chang, M. E., & Xu, M. (2017). Infrastructure ecology: An evolving paradigm for sustainable urban development. *Journal of Cleaner Production, 163*, S19–S27.
Paneru, S., Ghimire, P., Kandel, A., Kafle, S., & Rauch, C. (2024). Embodied residential building carbon emissions reduction in Nepal using linear optimization modeling. *Journal of Building Engineering*, Article 108531.
Pauliuk, S., Wang, T., & Müller, D. B. (2012). Moving toward the circular economy: The role of stocks in the Chinese steel cycle. *Environmental Science and Technology, 46*(1), 148–154.
Peled, Y., & Fishman, T. (2021). Estimation and mapping of the material stocks of buildings of europe: A novel nighttime lights-based approach. *Resources, Conservation and Recycling, 169*, Article 105509.
Peng, Z., Lu, W., & Webster, C. J. (2021). Quantifying the embodied carbon saving potential of recycling construction and demolition waste in the Greater Bay Area, China: Status quo and future scenarios. *Science of the Total Environment, 792*, Article 148427.
Qiao, W., & Huang, X. (2022). The impact of land urbanization on ecosystem health in the Yangtze River Delta urban agglomerations, China. *Cities, 130*, Article 103981.
Schiller, G., Gruhler, K., & Ortlepp, R. (2017). Continuous material flow analysis approach for bulk nonmetallic mineral building materials applied to the German building sector. *Journal of Industrial Ecology, 21*(3), 673–688.
Sen, P. K. (1968). Estimates of the regression coefficient based on Kendall's tau. *Journal of the American Statistical Association, 63*(324), 1379–1389.
Seto, K. C., Golden, J. S., Alberti, M., & Turner, B. L. (2017). Sustainability in an urbanizing planet. *Proceedings of the National Academy of Sciences, 114*(34), 8935–8938.
Suh, S., Lenzen, M., Treloar, G. J., Hondo, H., Horvath, A., Huppes, G., Jolliet, O., Klann, U., Krewitt, W., & Moriguchi, Y. (2004). System boundary selection in life-cycle inventories using hybrid approaches. *Environmental Science and Technology, 38*(3), 657–664.
Sun, J., Wang, T., Jiang, N., Liu, Z., & Gao, X. (2023). Gridded material stocks in China based on geographical and geometric configurations of the built-environment. *Scientific Data, 10*(1), 915.
Sutton, P. C. (2003). A scale-adjusted measure of "urban sprawl" using nighttime satellite imagery. *Remote Sensing of Environment, 86*(3), 353–369.
Tanikawa, H., Fishman, T., Okuoka, K., & Sugimoto, K. (2015). The weight of society over time and space: A comprehensive account of the construction material stock of Japan, 1945–2010. *Journal of Industrial Ecology, 19*(5), 778–791.
Tanikawa, H., & Hashimoto, S. (2009). Urban stock over time: Spatial material stock analysis using 4d-GIS. *Building Research & Information, 37*(5–6), 483–502.
Tanikawa, H., Hashimoto, S., & Moriguchi, Y. (2002). Estimation of material stock in urban civil infrastructures and buildings for the prediction of waste generation. *Proceedings of the fifth international conference on ecobalance*. Japan: Tsukuba.

Van Ooteghem, K., & Xu, L. (2012). The life-cycle assessment of a single-storey retail building in Canada. *Building and Environment, 49*, 212–226.
Vilaysouk, X., Islam, K., Miatto, A., Schandl, H., Murakami, S., & Hashimoto, S. (2021). Estimating the total in-use stock of Laos using dynamic material flow analysis and nighttime light. *Resources, Conservation and Recycling, 170*, Article 105608.
Wang, Z., Zhang, J., Luo, P., Sun, D., & Li, J. (2023). Revealing the spatio-temporal characteristics and impact mechanism of carbon emission in China's urban agglomerations. *Urban Climate, 52*, Article 101733.
Wiedenhofer, D., Fishman, T., Lauk, C., Haas, W., & Krausmann, F. (2019). Integrating material stock dynamics into economy-wide material flow accounting: Concepts, modelling, and global application for 1900–2050. *Ecological Economics, 156*, 121–133.
You, F., Hu, D., Zhang, H., Guo, Z., Zhao, Y., Wang, B., & Yuan, Y. (2011). Carbon emissions in the life cycle of urban building system in China—a case study of residential buildings. *Ecological Complexity, 8*(2), 201–212.
Zhang, X., Li, Y., Chen, H., Yan, X., & Liu, K. (2023). Characteristics of embodied carbon emissions for high-rise building construction: A statistical study on 403 residential buildings in China. *Resources, Conservation and Recycling, 198*, Article 107200.
Zhang, Q., & Seto, K. C. (2011). Mapping urbanization dynamics at regional and global scales using multi-temporal DMSP/OLS nighttime light data. *Remote Sensing of Environment, 115*(9), 2320–2329.
Zhang, L., Wu, P., Niu, M., Zheng, Y., Wang, J., Dong, G., Zhang, Z., Xie, Z., Du, M., & Jiang, H. (2022). A systematic assessment of city-level climate change mitigation and air quality improvement in China. *Science of the Total Environment, 839*, Article 156274.
Zhao, Y., Wang, S., & Zhou, C. (2016). Understanding the relation between urbanization and the eco-environment in China's Yangtze River Delta using an improved EKC model and coupling analysis. *Science of the Total Environment, 571*, 862–875.
Zheng, J., Jiang, P., Qiao, W., Zhu, Y., & Kennedy, E. (2016). Analysis of air pollution reduction and climate change mitigation in the industry sector of Yangtze River Delta in China. *Journal of Cleaner Production, 114*, 314–322.
Zheng, L., Mueller, M., Luo, C., Menneer, T., & Yan, X. (2023). Variations in whole-life carbon emissions of similar buildings in proximity: An analysis of 145 residential properties in Cornwall, UK. *Energy and Buildings, 296*, Article 113387.
Zheng, H., Wu, Y., He, H., Delang, C. O., Lu, J., Yao, Z., & Dong, S. (2024). Urbanization and urban energy eco-efficiency: A meta-frontier super ebm analysis based on 271 cities of China. *Sustainable Cities and Society, 101*, Article 105089.
Zhong, R., Pu, L., & Pei, F. (2024). A framework to assess the comprehensive sustainability of human consumption and production: A case study of the Yangtze River Delta in China. *Journal of Cleaner Production, 434*, Article 140049.
Zhou, W., Moncaster, A., O'Neill, E., Reiner, D. M., Wang, X., & Guthrie, P. (2022). Modelling future trends of annual embodied energy of urban residential building stock in China. *Energy Policy, 165*, Article 112932.
Zhou, C., Wang, S., & Wang, J. (2019). Examining the influences of urbanization on carbon dioxide emissions in the Yangtze River Delta, China: Kuznets curve relationship. *Science of the Total Environment, 675*, 472–482.